Journal of Materials Chemistry A

Accepted Manuscript

ROYAL SOCIETY OF CHEMISTRY

www.rsc.org/materialsA

Fabrication of antifouling, antimicrobial, well dispersed polydopamine functionalized halloysite nanotube-polyetherimide mixed matrix membranes for the heavy metal removal application

Raghavendra S. Hebbar[a], Arun M Isloor[a]*, K. Ananda[b]and A.F. Ismail[c]

[a]*Membrane Technology Laboratory, Chemistry Department, National Institute of Technology Karnataka, Surathkal, Mangalore 575 025, India.*
[b]*Biological Sciences, Poornaprajna Institute of Scientific Research, Bangalore 562110, India.*
[c]*Advanced Membrane Technology Research Center (AMTEC), UniversitiTeknologi Malaysia, 81310 Skudai, Johor Bahru, MALAYSIA*

Abstract

The polydopamine modified halloysite nanotube (HNTs) were synthesised through one step facile procedure and employed as a well dispersed hydrophilic additive to enhance the filtration properties of polyetherimide (PEI) membranes. The nanocomposite membranes were prepared by immersion precipitation method with different amount of modified HNTs (MHNTs) in the casting solution. The well dispersion of MHNTs throughout the membrane matrixwasconfirmed by elemental mapping analysis. The prepared nanocomposite membranes were extensively studied in terms of its porosity, morphology, membrane hydraulic resistance and hydrophilicity. The permeation experiments showed that, modified membrane exhibited higher water flux than pristine PEI membrane. The antifouling and anti-biofouling behaviour of the modified membranes was investigated in detail. The results revealed that, membrane with 3wt% of the MHNTs dosage showed higher Fouling Resistance Ratio (FRR) of 74.5% with reversible membrane fouling 64.3%. Moreover, the membrane showed excellent resistance to the microbial growth on the membrane surface. The well performed membrane was subjected to heavy metal ion rejection.Results indicated that, membranes were having the capacity to adsorb the Pb^{2+} and Cd^{2+}. Overall, PEI-MHNTs nanocomposite membranes could have great potential to improve the antifouling, anti-biofouling and the filtration properties.

Author for correspondence: E-mail address: isloor@yahoo.com, Fax: 91 824 2474033

1. Introduction

One of the most persuasive problems associated with scarcity of clean and fresh water across the globe are well known. The human health has been seriously affected by poor water quality and water related diseases.[1]The number of contaminants entering to the fresh water source increasing due to the development and rapid industrialisation. The present need is to develop more effective, low-cost and robust methods to disinfect and decontaminate water from source to point of use, without further stressing the environment or endangering human health.[2] The membrane based water purification technologies have a wide range of advantages in comparison to traditional purification methods. The membrane related process are embedded with key features like no phase change, low energy consumption, easy integration and scale up.[3-4]

Polyetherimide (PEI) is one of the favourable membrane material because of its excellent film forming ability, mechanical strength and chemical resistance as well as low cost.[5] However, prepared membranes are inherently hydrophobic in nature, which enhances the resistance to water permeation by fouling and reduce the life time during the process. Since, hydrophobic membranes are inadequate for use in water treatment applications.Fouling is one of the major and significant issue faced in membrane separation process. The colloids, organics and organisms in the feed solution are prone to adsorb or deposit onto membrane surfaces and into pores, leading to fouling.[6]The available literatures reveal that, fouling by organic substances can eventually bring about changes in membrane hydrodynamic permeability and properties.[7-8]In addition, the membranes are susceptible to one more severe problem called bio-fouling, particularly when the membranes were employed in drinking water, wastewater treatment and water reclamation applications. Bio-fouling leads to the formation of a biopolymer matrix called as biofilm at the membrane surface.[9]This brings down membranes performance, thereby increasing the need for the frequent cleaning and maintenance. Thus adds more cost to the entire process. Moreover, bio-fouling is self-replicating in nature, thereby making it difficult to be eliminated by any pre-treatment. In addition to this, heavy metals present in the water constitute the most hazardous environmental pollutants in nature. Even lower concentrations of these pollutants accumulated in tissues of an organism cause severe and fatal damage to the health due to their extreme toxicity.[5]

Clay nanotubes are new prospective fillers for polymeric composites due to their large surface area, high length-to-diameter (L/D) ratio, good physico-chemical properties and low cost.[10]In particular, hallyosite, a type of naturally occurring clay material with a nanotubular structure (Fig.1). This consists of 1:1 aluminosilicate layer with abundant Si-OH and Al-OH groups, which endow halloysite nanotubes (HNTs) with net negative charge, strong hyrophilicity and facile modification ability. Compared with other nanosized materials, naturally occurring HNTs are easily obtained and much cheaper than other nanoparticles such as carbon nanotubes (CNTs), boron nitride nanotubes and other nanotbes . Hence, HNTs may have the potential to replace the expensive CNTs as hydrophilic additives.[11]Zhang et al. studied the effect of modified HNTs on the performance of the polyethersulfone (PES) ultrafiltration membrane. The results revealed that, the permeation properties of the hybrid membranes were significantly superior to the pure PES membrane, especially when the modified HNTs content was 3%; the pure water flux of the membrane reached the maximum at 396.5 $Lm^{-2}h^{-1}$. [12]Wang et al. investigated the influence of halloysite nanotubes grafted with 2- methacryloyloxyethyl phosphorylcholine (HNTs-MPC) on the performance and antifouling behaviour. The membrane exhibited significant improvement in the hydrophilicity and antifouling properties. [13]

Figure-1

Recently, Messersmith et al. described the facile and versatile modification technique using dopamine as a powerful modifier.[14]Dopamine is a kind of catecholamine that contains both catechol and primary amine functional groups. Under oxidizing conditions, dopamine is able to undergo self-polymerization in aqueous solution gives polydopamine (PDA). Jiang et al. stated that, PDA could strongly adhere into many solid substrate such as TiO_2 nanoparticles, graphene oxide, and clay materials.[15]Liu et al. enlightened that,the polar groups in PDA layer such as hydroxyl and amine groups, provide the substrates with improved hydrophilicity and antifouling ability. And also enhance the interfacial interactions between nanomaterials and polymer matrices.[16]Zhang et al. reported that, PDA binding method not only provides a strong binding force, but also enhance the membrane performance.[12]According to Gao et al.abundant functional groups of polydopamine functionalized graphene showed high adsorption capacities toward a wide spectrum of contaminants, including heavy metals, synthetic dyes and organic pollutents.[17]Since inherent hydrophilicity of the PDA coating provides desirable surface characteristics without the need

for further modification. However, so far, only limited information on the application of PDA modification is available.

In the current study, well dispersed HNTs modified with PDA was synthesised through one step facile procedure and used as hydrophilic additive to modify the PEI membranes. The PEI/MHNTs nanocomposite membranes were prepared by diffusion induced phase separation method with different amount of additive dosage. Effect of additive on the on membrane structure and performance were analysed in detail. Dynamic water contact angle measurement was used to characterize membrane surface hydrophilicity. The scanning electron microscopy (SEM) were used to investigate membrane surface and cross-sectional morphology. The presence of MHNTs and its uniform distribution in membrane matrix was confirmed by elemental analyses. The performance of modified membranes was studied in terms of water uptake capacity, water flux and membrane hydraulic resistance. Furthermore, antifouling, anti-biofouling and heavy metal ion rejection behavior was investigated in detail.

2. Materials and methods

2.1. Materials

Polyetherimide (PEI) (Mw = 35,000 Da), was obtained from Sigma Aldrich (India). The solvent N-methyl pyrrolidone (NMP) was purchased from Merck, India. Halloysite nanotube and dopamine were supplied by Sigma Aldrich.Tris(hydroxymethyl)aminomethane (99%) obtained from Alfa Acear. Bovine Serum Albumin (BSA) was procured from Central Drug House (CDH). The polyvinylpyrrolidone (PVP) was purchased from Sigma Aldrich, India.

2.2 Preparation of Modified HNTs.

The chemical modification of HNTs was carried out using reported procedure in the literature.[18]In brief, the calculated amount of HNTs was dispersed in demineralised water using ultrasound treatment for 0.5hrs to get a HNTs suspension (10 mg/mL, 50 mL). Then adjusted the pH value of the suspension to alkalescence (pH 8.8) by using the base tris(hydroxymethyl)aminomethane. Afterwards,0.2 mg/mL of dopamine powder was added into the HNTs suspension being stirred at 30 °C. The obtained solution was continuously stirred for 6hrs to get HNTs coated with black insoluble polydopamine polymer (Fig.2). The resulting product was collected by centrifugation and washed with distilled water repeatedly until the black filtrate became colourless.

Figure-2

2.3. Preparation of composite membrane

PEI/MHNTs mixed matrix membranes were prepared by non-solvent induced phase separationmethod. [19]The calculated amount of MHNTs (0 wt% to 4wt% of PEI dosage) was dispersed in suitable volume of NMP solvent and stirred for 90 minutes at ambient temperature. The desired quantity of PEI (overall 20 wt% of polymer concentration mentioned in the final casting solution) was added to the above dispersed solution along with 2% of invariable pore forming agent PVP. Then the solution was stirred for 18 hrs at 65° C to obtain homogeneous casting solution. The obtained solution was kept for few hours without stirring at same temperature to get rid of trapped air. The casting solution was spread ona clean glass plate and casted using doctor's blade. Then it was immersed into a water bath and allowed to stand in coagulation bath for 24 hrs to ensure complete phase inversion. Overviews of compositions of the membranes were described in Table 1.

Table-1

2.3. Membrane characterization

2.3.1. FTIR analysis

The chemical modification of the HNTs were analysed by FTIR spectrum. The FTIR spectra were recorded using Avatar 360 IR spectrophotometer in the range of 4000-500 cm^{-1}. The changes in the characteristic peaks of spectra have been discussed in results and discussion.

2.3.2. TEM analysis

The TEM images of halloysite nanotube (HNTs) and modified halloysite nanotube (MHNTs) were recorded using JEM 1230 Electron Microscope. A small amount of HNTs and MHNTs was dispersed in ethanol using a bath sonicator for 20 min. A small amount of the suspension was then dropped onto a copper grid. After 16hrs, the grid was placed into the TEM for analysis.

2.3.3. Morphology of the membranes

The surface and cross sectional SEM images of the prepared composite membranes were recorded by Joel JSM-6380LA scanning electron microscope. The membrane samples were fractured cryogenically by dipping in liquid nitrogen for 1min and sputtered with a thin layer of gold using a sputtering apparatus. Also the X-ray elemental mapping analysis of

alumina and silicon on the membrane surface was performed to understand the distribution of MHNTs.

2.3.4. Water uptake and contact angle measurement

The water uptake capacity of the membrane is an important parameter to know about its bulk hydrophilicity. Briefly, the dry membranes were cut into 2 cm^2 size and weighed. These membrane samples were soaked in distilled water for 24hrs and weighed after wiping with blotting paper. The percentage water content in the membrane was calculated using equation (1)

$$\%\ uptake = \left(\frac{W_w - W_d}{W_w}\right) X100 \qquad (1)$$

Where W_w and $W_d$are the membrane weights after swelling for 24 hrs under wet and dry conditions respectively.

The change in the hydrophilicity of the prepared membranes after the addition of MHNTs was confirmed by measuring the water contact angle. The surface hydrophilicity was measured by FTA-200 Dynamic contact angle analyser by sessile droplet method. In order to minimize the experimental errors, the WCA measurement of each sample was measured three times and the average value was reported.

2.3.5 Membrane porosity

Porosity of the prepared nanocomposite membranes were calculated as mentioned in the literature by Zhang et al.[20]In brief, the membrane (2 cm^2) was immersed in distilled water for 24 hrs. The weight of the wet membrane was noted as W_w,after carefully blotting the surface adhering water. Then, the wet membrane was placed in an air-circulating oven at 75° C for 24 hrs prior to measure the dry weight, W_d. The porosity of the prepared membranes were calculated using equation (2).

$$\varepsilon\ (\%) = \frac{W_w - W_d}{A \times l \times \rho} \times 100 \qquad (2)$$

Where, $'\varepsilon'$ is the porosity of membrane, $'\rho'$ is the density of pure water (0.998 g/cm^3), 'A' is the area of membrane (cm^2) and $'l'$ is the thickness of membrane (cm^2).

2.3.6 Membrane hydraulic resistance (R_h)

To determine membrane hydraulic resistance, the PWF of the prepared membranes was evaluated at different transmembrane pressure (TMP) viz 200, 400, 600, 800 and 1000

kPa. The hydraulic resistance (R_h) was calculated from the inverse of slope, using the equation (3)

$$R_h = \frac{\Delta P}{J_w} \qquad (3)$$

Where $J_w$is the pure water flux (L/m^{2}h), ΔP (KPa) is the pressure difference and $R_h$is the membrane resistance (KPa/Lm^{-2}h^{-1}).

2.3.7. Water flux study

Dead end filtration cell was used to determine the permeation properties of the membranes. The filtration experiments were performed on circular membrane disk with effective filtration area of 5cm^2. The feed tank was filled with test solution and pressured as per requirement. Each membrane was compacted at 0.4MPa pressure for 30 min before commencing the experiment. After 30 min, distilled water passed through the membrane for 80 min at 0.3MPa pressure to obtain pure water flux J_w (L/m^{2}h). The flux was calculated according to formula (4).

$$\mathrm{J_w} = \frac{\mathrm{Q}}{\Delta \mathrm{t\ A}} \qquad (4)$$

Where, J_w is PWF and 'Q' is the amount of water collected for Δt (h) time duration using a membrane of area A (m^2).

2.3.8. Antifouling properties

The antifouling behaviour of all the prepared membranes was analysed using the reported procedure as in the literature.[19]In brief, each membrane was subjected to compaction for an initial 30 min at 0.4 MPa. Then the pressure was reduced to 0.3MPa and PWF of the membrane was determined J_{w1}(L/m^{2}h) at 0.3MPa TMP. The BSA solution was prepared with concentration of 0.8 g/L and passed through the membrane. After BSA filtration, membrane couponwas flushed with distilled water to remove loosely adhered protein molecules. PWF of cleaned membrane was noted as J_{w2} (L/m^{2}h). The antifouling behaviour of the membranes were determined in terms of flux recovery ratio (FRR) using the equation (5).

$$FRR(\%) = \left(\frac{J_{w2}}{J_{w1}}\right) X\ 100 \qquad (5)$$

Generally, higher FRR signifies a better antifouling behaviour of the membranes. Also, in order to examine the fouling processes, following studies were carried out. To estimate the total protein fouling (R_t) produced by the membrane after BSA filtration was calculated by equation (6).

$$R_t(\%) = \left(\frac{J_{w1} - J_p}{J_{w1}}\right) \times 100 \quad (6)$$

The flux loss caused from both reversible and irreversible protein fouling (R_r and R_{ir}), which were calculated using equation (7) and (8)

$$R_r(\%) = \left(\frac{J_{w2} - J_p}{J_{w1}}\right) \times 100 \quad (7)$$

$$R_{ir}(\%) = \left(\frac{J_{w1} - J_{w2}}{J_{w1}}\right) \times 100 \quad (8)$$

2.3.9 Heavy metal ion rejection study

Polymer enhanced ultrafiltration (PEUF) and ultrafiltration (UF) experiments were carried out to analyse the heavy metal ion rejection behaviour of the prepared membranes. The aqueous solution of lead nitrate and cadmium nitrate were prepared in presence of 1wt% of polyethyleneimine with initial concentration of 1000ppm. The pH of the resultant solution was adjusted to 6±0.5 by using 0.1M HCl or 0.1M NaOH solution. The obtained solution was stirred for 5 day in room temperature in order have complete binding between metal ion and polyethyleneimine. The heavy metal ion rejected by the membrane was determined by measuring the metal ion concentration in the feed and permeate by using the AAS (Atomic Absorption Spectrometer). The percentage of metal ion rejected by the membrane was calculated by using the formula (9)

$$\%\mathrm{R} = \left(1 - \frac{C_p}{C_f}\right)\mathrm{x}100 \quad (9)$$

Where, C_p and C_f are the concentration of heavy metal ion in the permeate and feed respectively.

2.3.10 Antimicrobial property of the membrane

Antimicrobial property of the MHNTs modified membrane was investigated by inhibition of microbial growth according to the literature.[15] In brief, the standard cultures of three bacteria *Mycobacterium smegmatis* (MTCC 994), *Staphylococcus aureus* (MTCC3160) and *Escherichia coli* (MTCC1687) and fungi *Candida albicans* (MTCC 7253) was obtained from IMTECH, Chandigarh, India. Microbial cultures were grown in nutrient agar media and sub cultured into nutrient broth. Hundred microlitre of microbial culture (0.5 Mac Farland) was spread on the agar plate using a cotton bud. Membranes were cut into about 9 mm disc

like pieces and placed on microbial mat with active surface facing the culture. Incubated the plates for 12 hours and observed for the zone of inhibition. Standard Fluconazole and Ciprofloxacin prepared at 10 mg/mL concentration was used as reference standards for fungi and bacteria respectively.

Another set of experiment was carried out to check the anti-biofouling capacity of the membranes by incubation method. In brief, membranes were cut into 1 cm x 3 cm size strips and incubated in 100 times diluted 0.5 Mac Farland microbial culture in a test tube for 12 hours. Sterile whatman filter paper strip of similar size was used as control. After 12 hours of incubation, all the strips were taken out, drained and placed on nutrient agar plates. Agar plates are observed for the microbial colonies around the membranes.

3. Results and discussion

3.1Characterization of HNTs and DHNTs.

3.1.1 TEM

The representative TEM images of the pristine HNTs and MHNTs were displayed in Fig.3. The image Fig.3a revealed that, HNTs possess a tubular structure with open end in the either side. The lengths of the HNTs varies from 150nm to 600nm and the thickness in the range of 30nm to 90nm. The change in the morphology of the MHNTs elucidated by measuring the diameters of nanotubes before and after modification from TEM images. The tubular structure of MHNTs becomes thicker than that of HNTs (Fig.3b). After modification, thickness of the MHNTs increased to about 15-20nm compared to virgin HNTs. This indicating that, a polydopamine polymer layer had formed on the surface of the HNTs. Similar result for the polydopamine modification of the HNTs were reported by the Chao et al.[20]

Figure-3

3.1.2 FT-IR analysis

The Fig.4 represents the FT-IR spectrums of HNTs and MHNTs. The spectrum of HNTs showed an absorption peaks at 3688cm^{-1} and 3618cm^{-1} due to the stretching vibration of –OH groups. The peak at 913cm^{-1} represents the bending vibration of Al–OH bond. The spectral band at 1022cm^{-1} corresponding to the stretching vibration of Si–O bonds. After modification of HNTs, the spectrum displayed broad peak at 3422cm^{-1} corresponding to the –OH groups of the polydopamine. Also, the peak at 3615cm^{-1}and 3688cm^{-1}ascribed to symmetric and asymmetric stretching vibration of –NH groups respectively.[18]The absorption band at

1624cm^{-1} corresponding to the carbonyl group of polydopamine. This confirms the formation of the polydopamine coating on the HNTs.

Figure-4

3.2 Hydrophilicity of the membranes

The hydrophilicity of the membrane is one of the important parameter for water treatment application.It can be explained by water swelling test and water contact angle measurement. The water uptake capacity of the membrane depends on number of hydrophilic sites on the membrane matrices and on the membrane morphology i.e presence of macro-voids in the sub-layer.[21]The water uptake capacity of all prepared membranes has been presented inFig.5. The membrane with 0 wt% of MHNTs showed around 58.4 % of water uptake capacity and it increases as the MHNTs content increased in the membrane matrix. This is the direct indication of increase in number of hydrophilic sites in membrane matrix and also observed that, increased macro voids in the sub-layer of the membrane.

Figure-5

Generally, the water contact angle (WCA) measurement is used to estimate the hydrophilicity and wetting characteristics of the membranes (Fig.5). A larger value of WAC symbolises a hydrophobic surface, whereas a smaller WCA indicates a hydrophilic surface. The HMM-0 membrane had showed a contact angle value of about 79.1°, whereas membrane with 4wt% of MHNTs dosage in the membrane matrix showed contact angle of 66.3°. This implies that, the hydrophilicity of the membrane surface had been improved significantly due to the addition of the MHNTs. This result could be explained due to the fact that, during the phase inversion process, hydrophilic MHNTs inclined to migrate spontaneously towards the top surface to reduce the interface energy. The top surface photographs of prepared membranes are represented in Fig.6. The results illustrate that, the surface of the membrane was darker as increase in the MHNTs dosage. Therefore, hydrophilic MHNTs presented on the membrane surface were easily susceptible to wet and adsorbed by water, giving rise to lower water contact angle. Some related articles reported the similar phenomena for the additives such as graphene oxide (GO), TiO_2 nanoparticles and carbon nanotube (CNTs).[22-23]

Figure-6

3.3 Porosity of the membrane

It is generally accepted that, performance of asymmetric membranes is predominantly controlled by the skin layer whereas, the supporting layer has only a minor influence. This indicates that, the rejection and the intrinsic permeation properties of the membranes depends on porosity or pore size distribution. There was a significant change in the porosity and morphology of membranes was observed with different amount of MHNTs dosage. From the literature, it was observed that, adding different amounts of inorganic additives such as TiO_2, clay, CNTs, graphene oxide etc. in to the casting solution, alters the performance of the resulting membranes.[5, 22-23]The porosity of the PEI/ MHNTs nanocomposite membranes was displayed in Table-2. The results revealed that, all PEI/MHNTs nanocomposite membranes have exhibited higher porosity than HMM-0 membrane. However, with increasing MHNTs content, membrane porosity increases first and then decreases. This is due to the addition of MHNTs into the casting solution enhance the inflow rate of non-solvent i.e water and at the same time hindered the exchange process between solvent and non-solvent during the phase separation process. This enhance the ratio of water content in the nascent membrane and increased the porosity. Also a portion of PVP was leached out of the casting film during the exchange of solvent−nonsolvent process and acted as a pore-former during membrane formation, which may be another reason for the enhancing the membrane porosity. [24]

Table-2

3.4 Morphological study

It is generally known that, surface and cross sectional image of the membrane having the significant part in identifying the role of morphological feature on permeability and rejection behaviour. [25]In order to investigate the influence of MHNTs on the morphology of the prepared membrane by using the SEM and representative image was shown in the Fig.7. All the membranes showed typical asymmetric structure with compact top layer and porous sub-layer (fully developed macropores at the bottom). The addition of MHNTs into the casting solution with increasing MHNTs content in the composite membrane, the number of macrovoids increases in bottom layer and the pore walls among macrovoids become looser with some channel-like pores. During operation, the skin layer would offer high resistance to the material transport and bottom sub-layer would offer less resistance to the material transport besides offering mechanical strength to the membrane. Further elemental mapping of silicon and aluminium was carried out in order to confirm the presence and uniform distribution of the MHNTs in the membrane (Fig.8).

From the literature it was observed that, presence of inorganic additives in the membrane dope having significant influence on the membrane morphology.[26]After addition of hydrophilic MHNTs additive into the casting solution alters the kinetics and thermodynamic behaviour during phase inversion process. It has also been reported that, presence of inorganic additives in the casting solution reduce the interaction among the polymer chain. On the other hand due to hydrophilic nature of the MHNTs, there is a possibility of formation of hydrogen bond with solvent N-Methyl-2-pyrrolidone (NMP). Since rate of non-solvent (water) inflow increases and solvent (NMP) outflow decreases. Consequently slower the transport of solvent/ non-solvent across the cast film in the coagulation bath during the membrane formation process. This resulted formation of a dense top layer and the formation of macro-voids (finger-like pores) in the bottom layer is improved.[27]

Figure-7

Figure-8

3.5 Permeation properties

The time dependent pure water fluxes (PWF) of the prepared membranes at 0.3 MPa pressure was showed in Fig.9. It can also be observed that, gradual decrease in the PWF of membranes during membrane compaction. Compaction is described as a compression of membrane structure under a transmembrane pressure (TMP) difference causing a reduction in membrane permeability. Usually, this compression reflects a reduction of membrane thickness due to mechanical deformation.[24, 28]Peterson et al. studied the membrane compaction by an ultrasonic time domain reflectometry (UTDR) technique. The results revealed that, the membrane with high porosity experienced higher initial compression strain than that of low porosity.[29]In present work, the pure water flux of HMM-0 membrane decreased from 149 $Lm^{-2}h^{-1}$ to 125 $Lm^{-2}h^{-1}$, whereas HMM-2 membrane exhibited flux reduction 276 $Lm^{-2}h^{-1}$ to 245 $Lm^{-2}h^{-1}$ during membrane compaction. Compared with PEI/MHNTs nanocomposite membranes, HMM-0 membrane displayed a less reduction in the flux, which may be due to its low porosity and less number of macrovoids in the sublayer. After about 30 min of membrane compaction, the PWF of the membranes reached a steady state. The decline in the water flux during membrane compaction becomes more severe with the addition of MHNTs in the membrane matrix. This may be due to the presence of lots of macro-voids in the sub-layer of PEI/MHNTs nanocomposite membranes.

Figure-9

From the permeation experiment it was clear that, all the modified membrane exhibited significantly superior PWF compared to pristine PEI membrane. With increasing MHNTs dosage in the membrane, the PWF increased first and then decreased. This can be explained by the changes of membrane morphology, porosity and hydrophilicity. When MHNTs content increased from 0 to 3wt %, the porosity, surface pore size, pore interconnection, macrovoids and hydrophilicity of the membrane was increased. Which significantly declining the resistance of water permeating through the membranes and thus increased membrane permeability. However, higher particle concentration (4wt %) in the membranes matrix lead to a decrease in PWF because of the pore blockage caused by excessive particles and the pore collapse in membrane cross-section resulted from aggregation of nanoparticles.

3.6 Membrane hydraulic resistance

The PWF of the nanocomposite membranes were measured at different transmembrane pressures (Fig.10). The membrane hydraulic resistances (R_h) were determined as the inverse of the slope of the plots of PWF against the respective transmembrane pressures.[30]The hydraulic resistance offered by the membranes with different amount of MHNTs shown in Table 2. The membrane showed decrease in the hydraulic resistance with increase in the MHNTs content in the membrane. The HMM-0 membrane showed hydraulic resistance of 1.59 Kpa/Lm^{-2}h^{-1} and it was observed to decline 0.88 Kpa/Lm^{-2}h^{-1} for the HMM-2 membrane. This can be explained by the fact that, the modified membrane consist of number of hydrophilic groups to enhance the hyrophilicity. When surface shows hydrophilicity, the water molecules forms weak secondary force interaction with the molecules of the surface. Due to this phenomenon, membrane easily became wet and exhibited less resistance to the water to pass through membrane. In addition to this, the presence PVP in the casting solution leads to formation of pores on the membrane surface. Since, increase in flux thereby decrease in membrane hydraulic resistance.

Figure-10

3.7 Antifouling performance of the membrane

It is well known that, membranes are highly susceptible to fouling during practical application, thereby greatly limiting their lifetime. Generally, the fouling caused by protein adsorption, which was resulted from the combination of electrostatic interaction, hydrogen

bonding effect, hydrophobic impact and Van der Waals force.[31]In fact, membrane fouling can be categorised as hydraulically reversible and irreversible membrane fouling. In case of hydraulically reversible fouling, the foulents are loosely bound or adhere to the membrane surface and can be easily detached by simple washing. Whereas in irreversible membrane fouling, the foulents are tightly attached to the membrane surface and can only be removed by chemical treatment.[32]In current study, BSA was used as a model protein to conduct the antifouling property study of the prepared membranes. Fig.11 shows the flux of the prepared membranes performed at 0.3 MPa pressure at 29°C in different conditions i.e. before BSA filtration, during BSA filtration and after BSA filtration. It can be seen that fluxes of all the membranes decrease rapidly during BSA ultrafiltration, which may be due to the deposition and absorption of BSA on membrane surface and pores.

Figure-11

The flux decline ratio and flux recovery ratio (FRR) of the prepared membranes were tabulated in Table 3. The FRR was as low as 26.6 % and total fouling ratio (R_t) of 92.1% was observed for the HMM-0 membrane. After addition of MHNTs in to the membrane matrix, the overall permeation FRR of the modified membrane reached up to 74.5%. The total fouling gradually decreased from 92.1% to 86.2 % for HMM-0 and HMM-2 membrane respectively. Particularly, HMM-2 membrane exhibited reversible fouling (R_r) up to 60.7% with flux rate of 168.7 L $m^{-2}h^{-1}$. Thus, the loosely adhered or adsorbed protein molecules on the membrane surface were easily detached by simple washing resulting in a high FRR. The results of flux decline behaviour and FRR values indicated that, modified membranes had better antifouling property as compared to HMM-0 membrane. This is because, the modified membrane consists of abundant number of hydrophilic functionality such as hydroxyl and amine groups, which induce the hydrophilicity to the surface. Since by minimizing strong hydrophobic–hydrophobic interactions between the foulants and membrane surface.[30]Further, hydrophilic nature of membrane surface are thought to attract a tightly bound layer of water molecules creating a buffer against the adhesion of foulants. Thus weakening the interactions of protein molecules with the membrane and reducing membrane fouling. Meanwhile, electrostatic repulsion between negatively charged BSA and membrane surface should also improve antifouling behaviour for hybrid membrane. The observed result is quite comparable with the polymer membrane consisting of hydrophilic modifying agents such as multiwalled carbon nanotubes, graphene oxide, nanoplates, silica and TiO_2 nanoparticles.[33-36]

Table-3

3.8 Heavy metal ion rejection study

The heavy metal ions are being environmentally persistent and non-biodegradable, they constitute the most hazardous environmental pollutants in nature.[37]Since in the present work, heavy metal ion rejected by the membranes were studied by both PEUF and UF experiments (Fig.12). The HMM-3 membrane exhibited rejection of 79% for Pb^{+2} ionsand 73% for Cd^{+2} ions respectively during the PEUF. The higher rejection of Pb^{+2} compared to Cd^{+2} was due to the ability of Pb^{+2} ion to form the larger size complex with polyethyleneimine complexing agent. Further, the % rejection of Pb^{+2} and Cd^{+2} during the normal UF (without complexing agent) were 34% and 27% respectively.This rejection behaviour due to adsorption behaviour by the membrane surface. In order to substanciate this, elemental mapping analysis of lead and cadmium were carried out on the membrane surface after the UF experiment (Fig.13).Since MHNTs inherently offers the negative charge to the membrane surface and presence of hydroxyl and amine groups on the polydopamine acts as chelating agents.[38]Thus, positively charged led and cadmium ions exhibits strong secondary force of interaction such as hydrogen bonding, dipolar interactions, electrostatic interactions etc. with the membrane surface (Fig.14). From the Fig.12, it was observed that, % of rejection offered by the PEUF was more compared to UF process. According to Valeen et al. the size of the complexed metal ion has larger than the membrane pores. Since complexed metal ions are retained in the feed solution. During the UF process, the most of the metal ions are easily pass through the membrane. Only metal ions adsorbed by the membranes contributed to the % of rejection.[23] Facile and efficient regeneration capacity of a process is an indicative parameter of environmentally as well as economically viable process. The reusability of the prepared membranes for heavy metal ion removal was investigated by treating 0.2 M nitic acid solution for 18 hrs. From the results we could observe that (table-4), modified membranes were able to remove almost same amount of heavy metal ion after acid treatment. This was further substanciated by elemental mapping analysis after acid treatment andwere presented in fig.15. This implied that modified membrane could be regenerated by simple acidtreatment.

Figure-12

Figure-13

Figure-14

Figure-15

3.9 Antimicrobial activity of membranes

There was a significant inhibition for *Escherichia coli*, *Mycobacterium smegmatis* and *Candida albicans* observed below the surface of the membranes, but no zone of inhibition observed around the disc for any of the microorganisms. The clear zone found below the membrane for *Escherichia coli*, *Mycobacterium smegmatis* and *Candida albicans* indicates membranes are inhibiting gram negative bacteria as well as fungi. There are few colonies were grown below the membrane for *Staphylococcus aureus* indicating less inhibition for gram positive bacteria. Inhibition of *Candida albicans* below the membrane and growth of few colonies of *Staphylococcus aureus* below the membrane are represented in the Fig.16. In addition to this, membrane incubation experiment showed very little or no microbial colonies were found around the membrane strips after 24 hours of incubation in microbial culture, whereas lot of the microbial colonies grown around the control strip (Fig.17).

These results indicate that, the modified membrane exhibited potential inhibition towards the growth of microorganisms on the surface. According to the Miller et al. more hydrophilic membrane surface could reduce the formation of biofouling.It has also been reported by the McCloskey et al. shown that the polydopamine coating has an effect on biofouling mitigation by enhancing the membrane hydrophilicity.[39]As stated above, the water contact angle of the active surface decreased with increasing MHNTs in the membrane. However, hydrophilicity was not the only reason for biofouling reduction in this study. The surface charge of the membrane has played a major influence on the antibiofouling properties. The Katsikogianni and Missirlis described that, almost all bacteria are negatively charged in aqueous suspensions, due to the existence of functional groups such as carboxyl and hydroxyl groups in cell wall components.[40]Electrostatic repulsion forces between bacteria and negatively charged membrane surface can be explained by calculating the interaction energy using the DLVO (Derjaguine-Landaue-Verweye-Overbeek) and XDLVO (extended DLVO) theories.[41]Furthermore, Park et al. also showed that more negatively charged membrane surfaces have more electrostatic repulsion forces with bacteria.[42]Based on this fact, it can be concluded that, MHNTs has a mitigating effect on the biofouling phenomena by enhancing hydrophilicity and surface negative charge.

Figure-16

Figure-17

4. Conclusion

Well dispersed hydrophilic MHNTs additives were prepared by using the facile and versatile polydopamine as modifying agent. The nanocomposite membranes were synthesized by immersion precipitation method with different amount of MHNTs dosage. The presence and uniform distribution of the additive into the membrane matrix was confirmed by elemental mapping. The results revealed that, modified membranes displayed enhanced porosity, water uptake capacity and hydrophilicity. The permeation experiments showed that, PWF of the nanocomposite membrane exhibited lower membrane hydraulic resistance (0.88 $Kpa/Lm^{-2}h^{-1}$) compared to HMM-0 membrane (1.59 $Kpa/Lm^{-2}h^{-1}$). The modified membrane exhibited superior antifouling behaviour with FRR of 74.5% and reversible fouling ratio of 60.7% for 3wt% of MHNTs dosage in the matrix. Also the modified membrane having the capacity to adsorb the heavy metal ion, thereby showing the rejection towards the Pb^{2+} and Cd^{2+}. Moreover, the modified membrane showed excellent resistance to microbial growth on the membrane surface. Overall, the well dispersed MHNTs is an effective additive to improve the membrane performance and it can be employed as a potential candidate for the further studies.

Acknowledgements AMI thank Prof. Swapan Bhattacharya, Director, National Institute of Technology Karnataka, Surathkal, India for providing the research facilities and encouragements. Authors also thank Prof K. Narayan Prabhu and Prof K. Rajendra Udupa of Metallurgical and Materials Engineering Department of NITK Surathkal, India for the contact angle measurements and SEM facility.

References

1. M. A. Shannon, P. W. Bohn, M. Elimelech, J. G. Georgiadis, B. J. Marinas and A. M. Mayes, Nature, 2008, **452**, 301-310.
2. H. W. Liang, X. Cao, W. J. Zhang, H. T. Lin, F. Zhou, L. F. Chen and S. H. Yu, Adv. Funct. Mater., 2011, **21**, 3851-3858.
3. J. Yin and B. Deng, J. Membr. Sci., 2014,
4. R. Kasher, Bulletin of the Israel Chemical Society, 2009, **24**, 10-18.
5. R. S. Hebbar, A. M. Isloor and A. Ismail, RSC Advances, 2014, **4**, 47240-47248.

6. D. Rana and T. Matsuura, Chem. Rev. (Washington, DC, U. S.), 2010, **110**, 2448-2471.
7. F. Xiao, P. Xiao, W. Zhang and D. Wang, J. Membr. Sci., 2013, 447, 144-152.
8. P. Xiao, F. Xiao, D.-s. Wang, T. Qin and S.-p. He, Sep. Purif. Technol., 2012, 95, 109-117.
9. K. Singh, P. Singh, S. Mishra and V. K. Shahi, J. Mater. Chem., 2012, **22**, 1834-1844.
10. H. Jing, Y. Higaki, W. Ma, J. Xi, H. Jinnai, H. Otsuka and A. Takahara, Polym. J. (Tokyo, Jpn.), 2014,
11. E. Abdullayev and Y. Lvov, J. Mater. Chem., 2010, **20**, 6681-6687.
12. J. Zhang, Y. Zhang, Y. Chen, L. Du, B. Zhang, H. Zhang, J. Liu and K. Wang, Ind. Eng. Chem. Res., 2012, **51**, 3081-3090.
13. Z. Wang, H. Wang, J. Liu and Y. Zhang, Desalination, 2014, **344**, 313-320.
14. H. Lee, S. M. Dellatore, W. M. Miller and P. B. Messersmith, science, 2007, **318**, 426-430.
15. J. Jiang, L. Zhu, L. Zhu, H. Zhang, B. Zhu and Y. Xu, ACS Appl. Mater. Interfaces, 2013, **5**, 12895-12904.
16. L. Liu, B. Shao and F. Yang, Sep. Purif. Technol., 2013, **118**, 226-233.
17. C. Chao, J. Liu, J. Wang, Y. Zhang, B. Zhang, Y. Zhang, X. Xiang and R. Chen, ACS Appl. Mater. Interfaces, 2013, **5**, 10559-10564.
18. S. Shenvi, A. Ismail and A. M. Isloor, Ind. Eng. Chem. Res., 2014, **53**, 13820-13827.
19. G. Zhang, S. Lu, L. Zhang, Q. Meng, C. Shen and J. Zhang, J. Membr. Sci., 2013, **436**, 163-173.
20. B. Ganesh, A. M. Isloor and A. Ismail, Desalination, 2013, **313**, 199-207.
21. S. Zinadini, A. A. Zinatizadeh, M. Rahimi, V. Vatanpour and H. Zangeneh, J. Membr. Sci., 2014, **453**, 292-301.
22. V. R. Pereira, A. M. Isloor, A. Al Ahmed and A. Ismail, New J. Chem., 2015,
23. S. Zhao, Z. Wang, X. Wei, B. Zhao, J. Wang, S. Yang and S. Wang, Ind. Eng. Chem. Res., 2012, **51**, 4661-4672.
24. S. Rajesh, K. H. Shobana, S. Anitharaj and D. R. Mohan, Ind. Eng. Chem. Res., 2011, **50**, 5550-5564.
25. P. Anadão, L. F. Sato, R. R. Montes and H. S. De Santis, J. Membr. Sci., 2014, **455**, 187-199.

26. H. Yu, Y. Zhang, X. Sun, J. Liu and H. Zhang, Chem. Eng. J. (Lausanne), 2014, **237**, 322-328.
27. J. B. Li, J. W. Zhu and M. S. Zheng, J. Appl. Polym. Sci., 2007, **103**, 3623-3629.
28. R. Peterson, A. Greenberg, L. Bond and W. Krantz, Desalination, 1998, **116**, 115-122.
29. J. Abdoul Raguime, G. Arthanareeswaran, P. Thanikaivelan, D. Mohan and M. Raajenthiren, J. Appl. Polym. Sci., 2007, **104**, 3042-3049.
30. H. Huisman, P. Prádanos and A. Hernández, J. Membr. Sci., 2000, **179**, 79-90.
31. X. Li, X. Fang, R. Pang, J. Li, X. Sun, J. Shen, W. Han and L. Wang, J. Membr. Sci., 2014,
32. V. Vatanpour, S. S. Madaeni, R. Moradian, S. Zinadini and B. Astinchap, J. Membr. Sci., 2011, **375**, 284-294.
33. H. Zhao, L. Wu, Z. Zhou, L. Zhang and H. Chen, Phys. Chem. Chem. Phys., 2013, **15**, 9084-9092.
34. M. Sun, Y. Su, C. Mu and Z. Jiang, Ind. Eng. Chem. Res., 2009, **49**, 790-796.
35. A. Sotto, A. Boromand, S. Balta, J. Kim and B. Van der Bruggen, J. Mater. Chem., 2011, **21**, 10311-10320.
36. X. Zou, G. Zhu, H. Guo, X. Jing, D. Xu and S. Qiu, Microporous Mesoporous Mater., 2009, **124**, 70-75.
37. Y. Yu, J. G. Shapter, R. Popelka-Filcoff, J. W. Bennett and A. V. Ellis, J. Hazard. Mater., 2014, **273**, 174-182.
38. D. J. Miller, P. A. Araujo, P. B. Correia, M. M. Ramsey, J. C. Kruithof, M. van Loosdrecht, B. D. Freeman, D. R. Paul, M. Whiteley and J. S. Vrouwenvelder, Water Res., 2012, **46**, 3737-3753.
39. M. Katsikogianni and Y. Missirlis, Eur Cell Mater, 2004, **8**, 37-57.
40. K.-Y. Kim, E. Yang, M.-Y. Lee, K.-J. Chae, C.-M. Kim and I. S. Kim, Water Res., 2014, **54**, 62-68.
41. N. Park, B. Kwon, I. S. Kim and J. Cho, J. Membr. Sci., 2005, **258**, 43-54.
42. H. Gao, Y. Sun, J. Zhou, R. Xu and H. Duan, ACS Appl. Mater. Interfaces, 2013, **5**, 425-432.

List of tables

Table-1 Composition of the casting solution

List of Figures

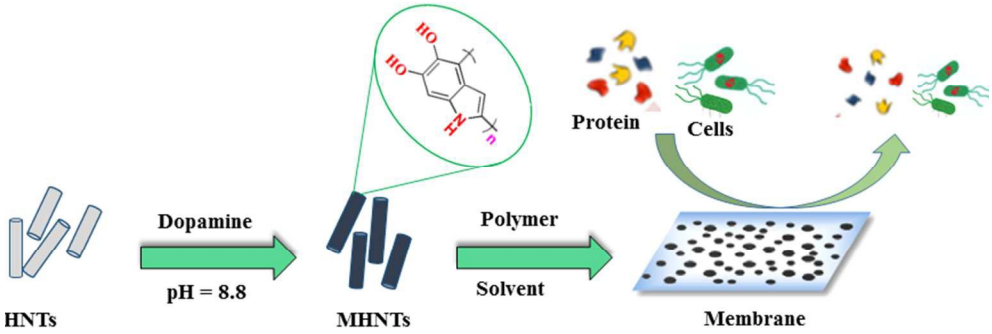

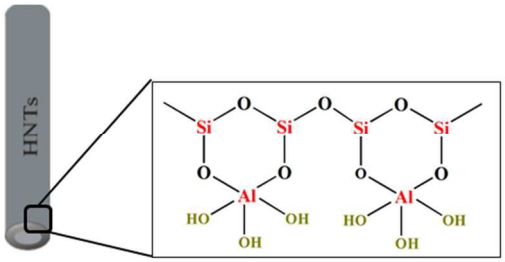

Fig.1 Chemical structure of halloysite nanotube [9]

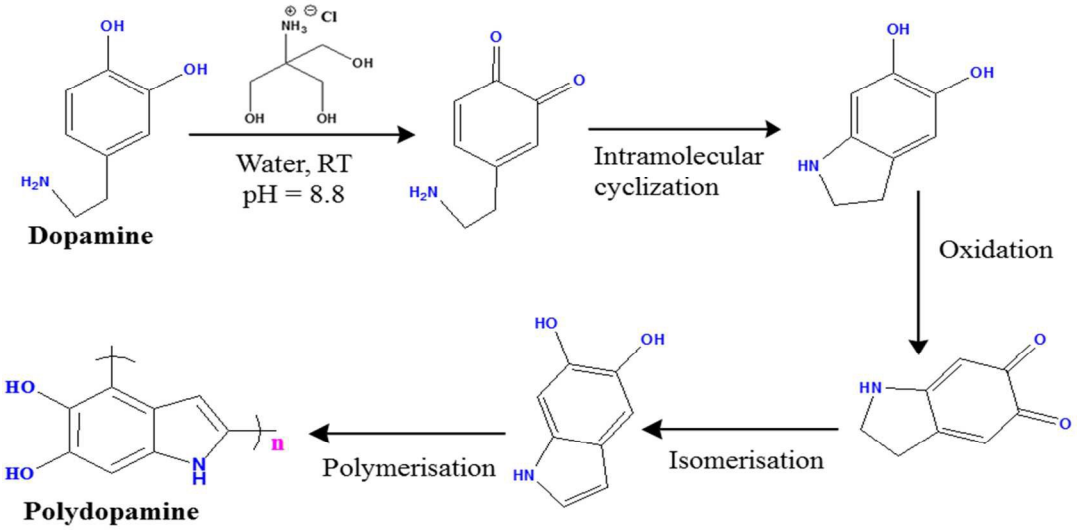

Fig.2 Schematic representation of polymerisation of dopamine

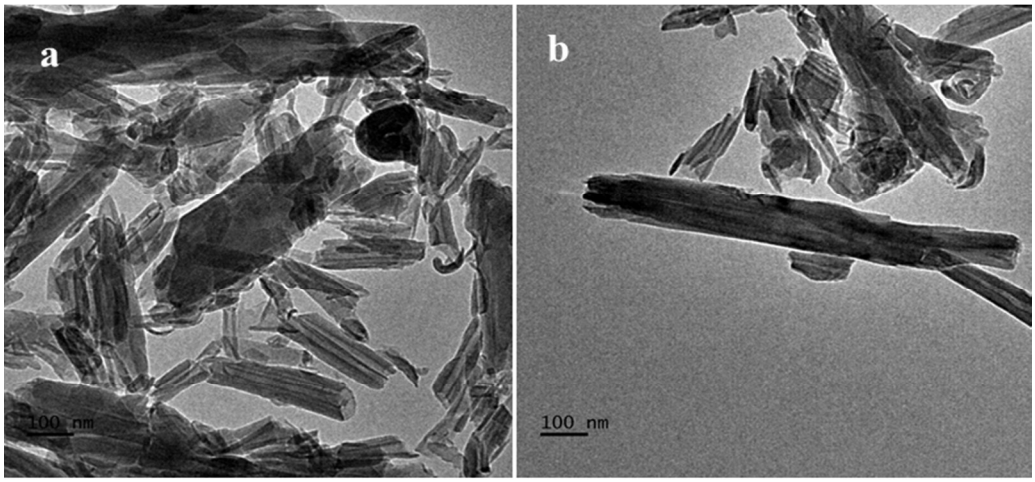

Fig.3 TEM images of a) HNTs and b) MHNTs

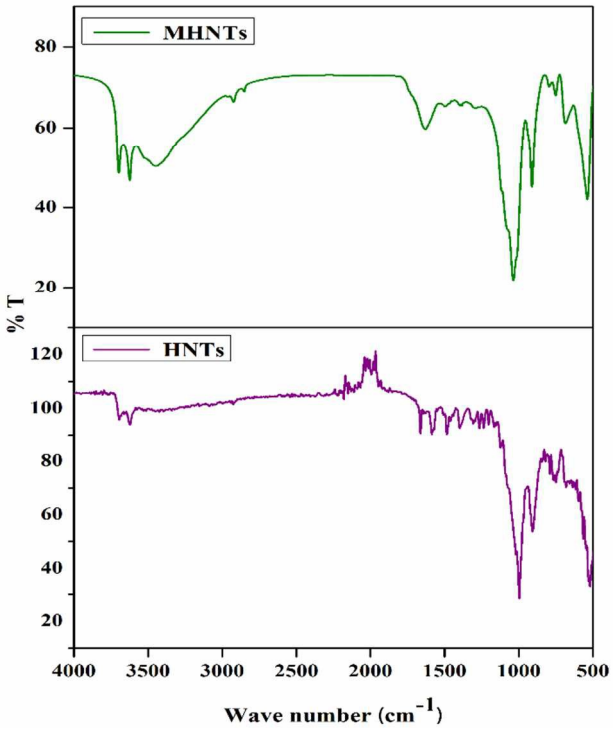

Fig.4 The FTIR spectrum of the HNTs and MHNTs

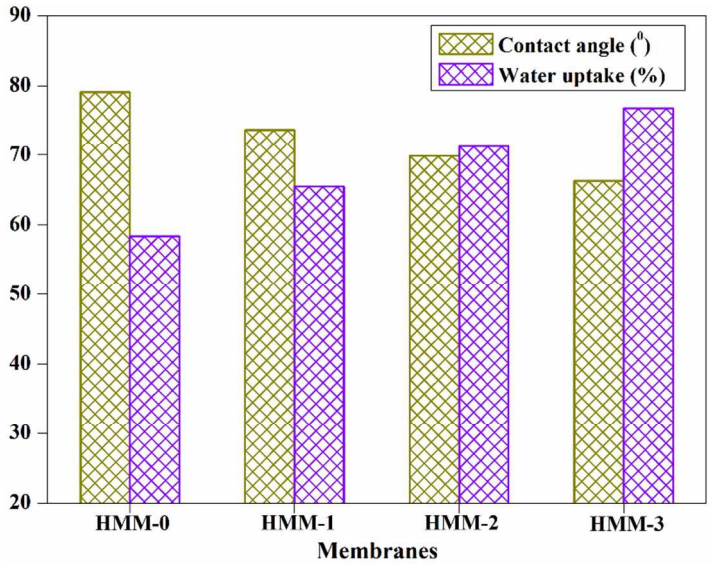

Fig.5 Contact angle and water uptake capacity of the membranes

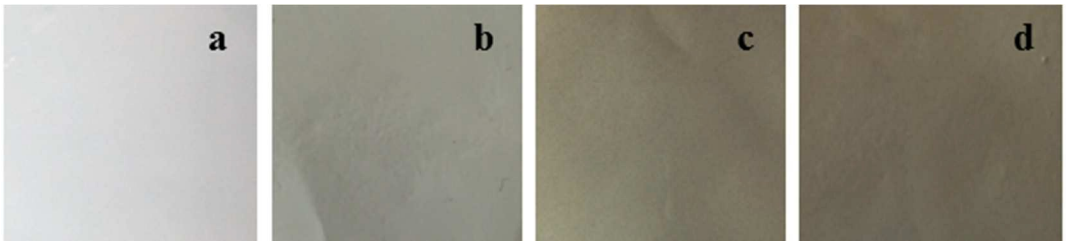

Fig.6 Digital photography of the top surface of a) HMM-0 b) HMM-1 c) HMM-2 and d) HMM-3 membranes

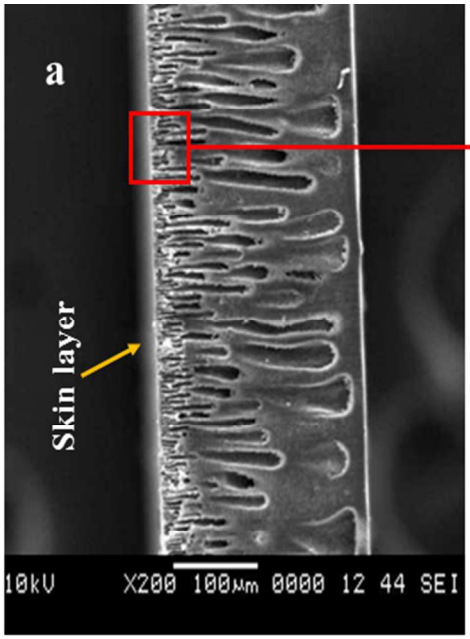

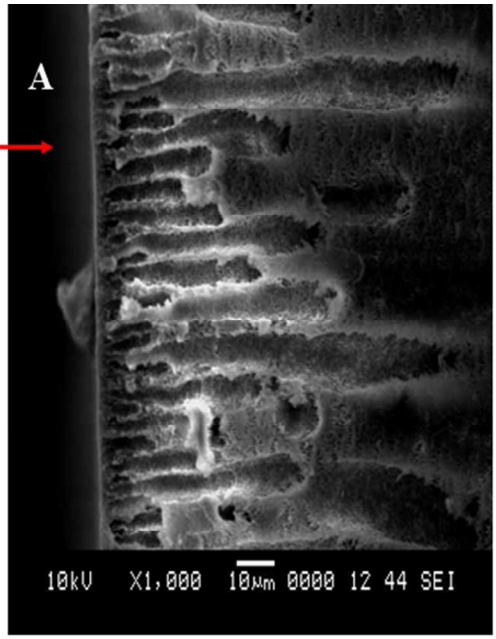

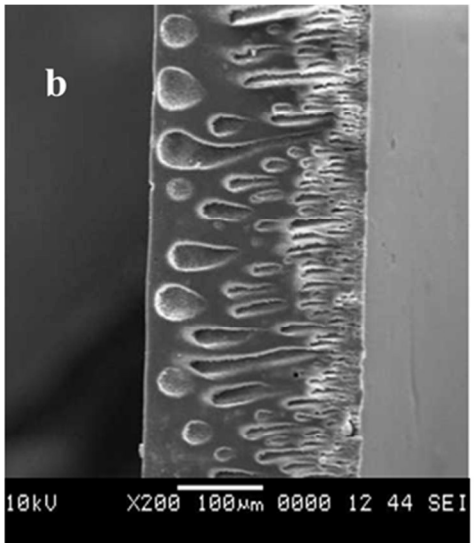

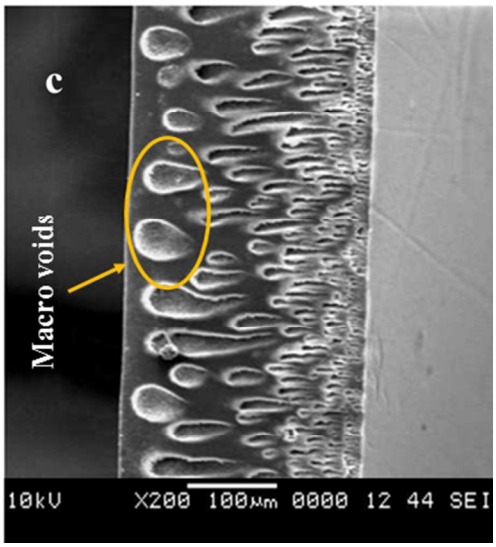

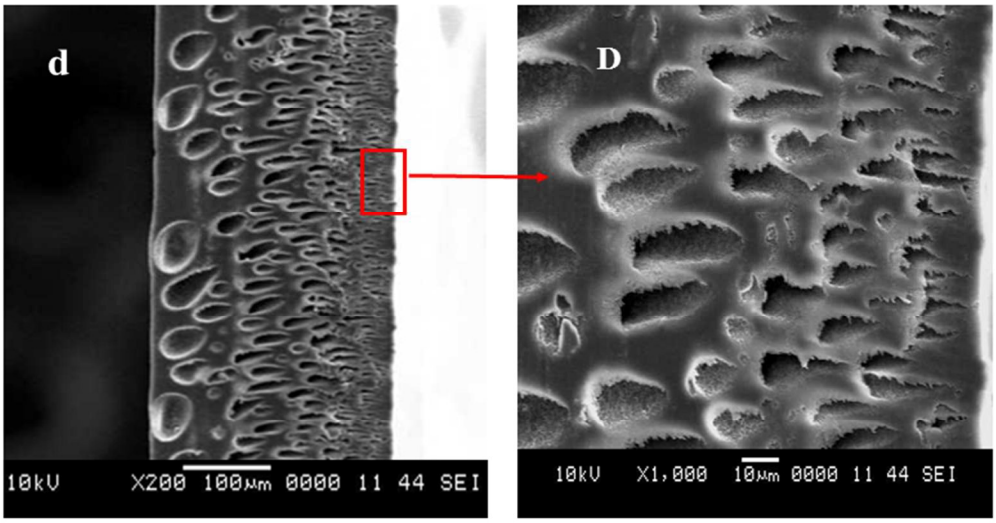

Fig.7 The cross sectional SEM images of the a) HMM-0, A) magnified HMM-0, b) HMM-1, c) HMM-2, d) HMM-3 and D) magnified HMM-3

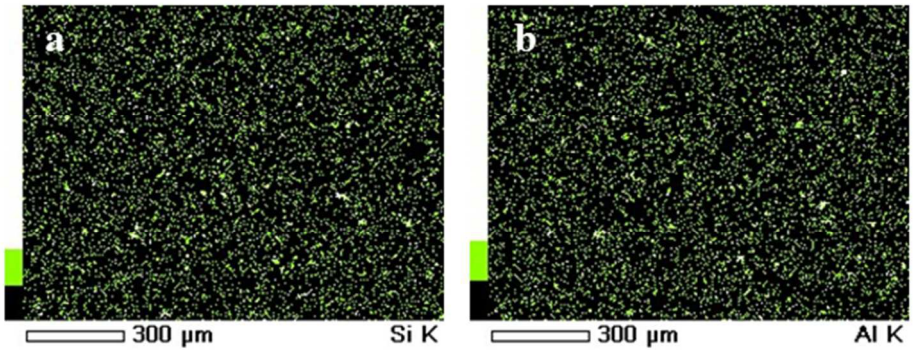

Fig.8 The elemental mapping of silicon and aluminium on HMM-2 membrane

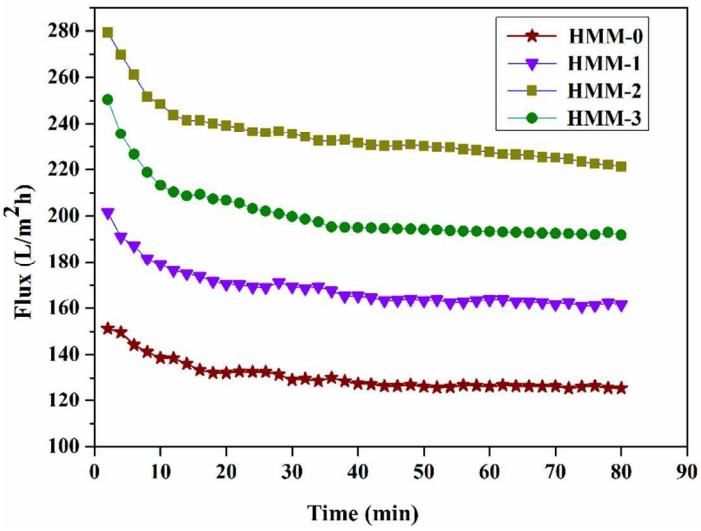

Fig.9 Time dependent pure water flux of the membranes

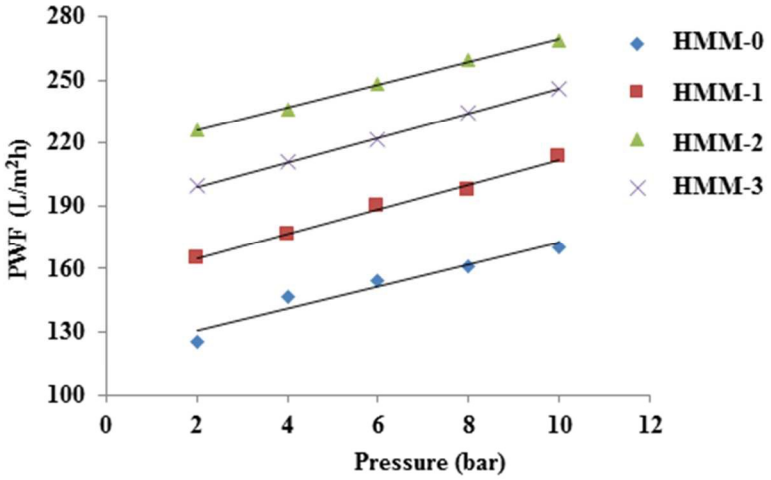

Fig.10 Pressure dependent pure water fluxes of membranes

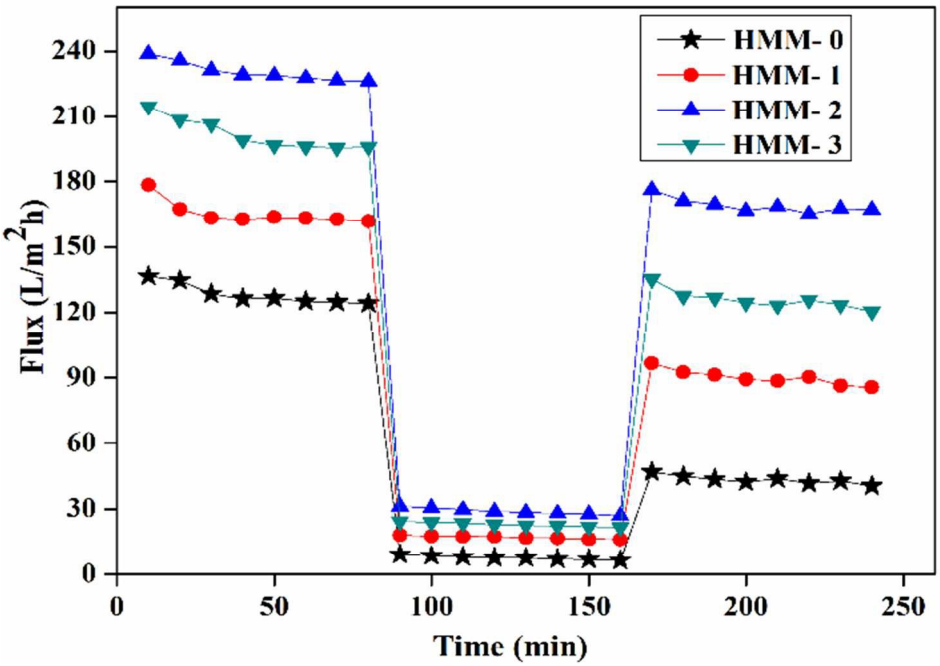

Fig.11 Flux versus time for membranes at 0.3 MPa during three conditions: water flux for 80 min, 0.8g/L BSA solution flux for 80 min, and water flux for 80min after through washing with distilled water

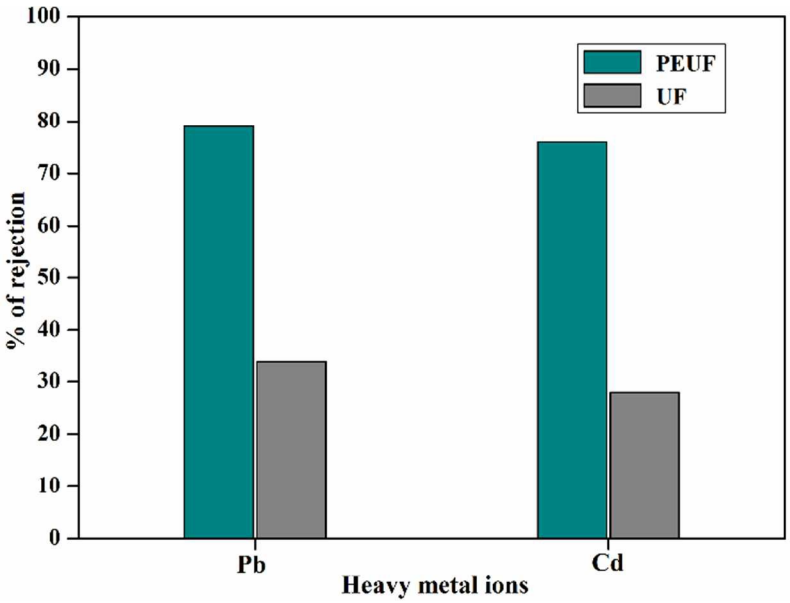

Fig.12 The heavy metal ion rejected by HMM-3 membrane

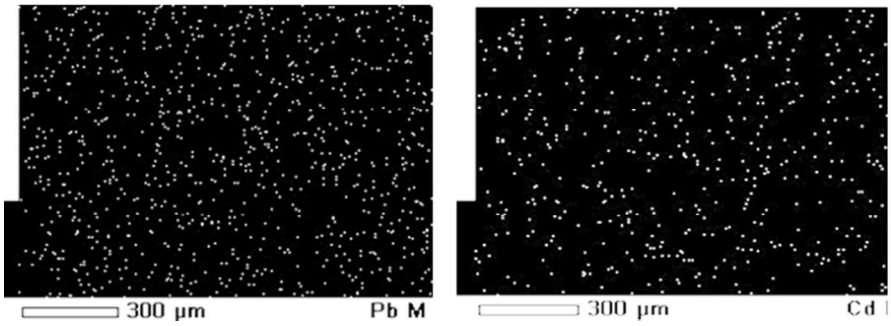

Fig.13 Elemental mapping of lead and cadmium after the UF experiment

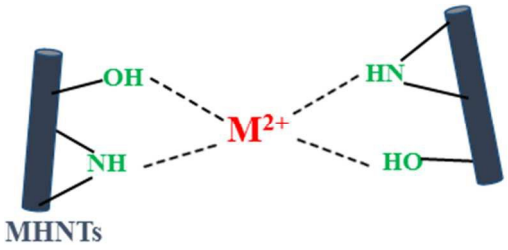

Fig.14 Interaction of heavy metal ion with MHNTs

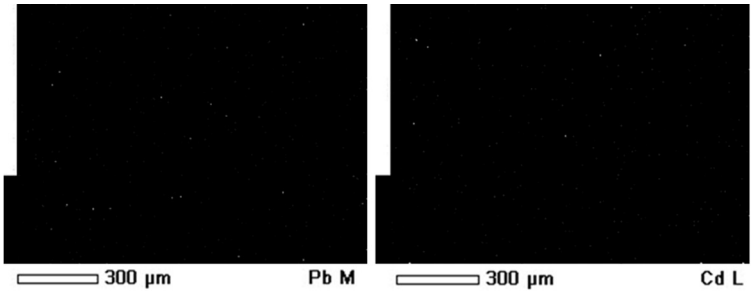

Fig.15 The elemental mapping of lead and cadmium after acid treatment.

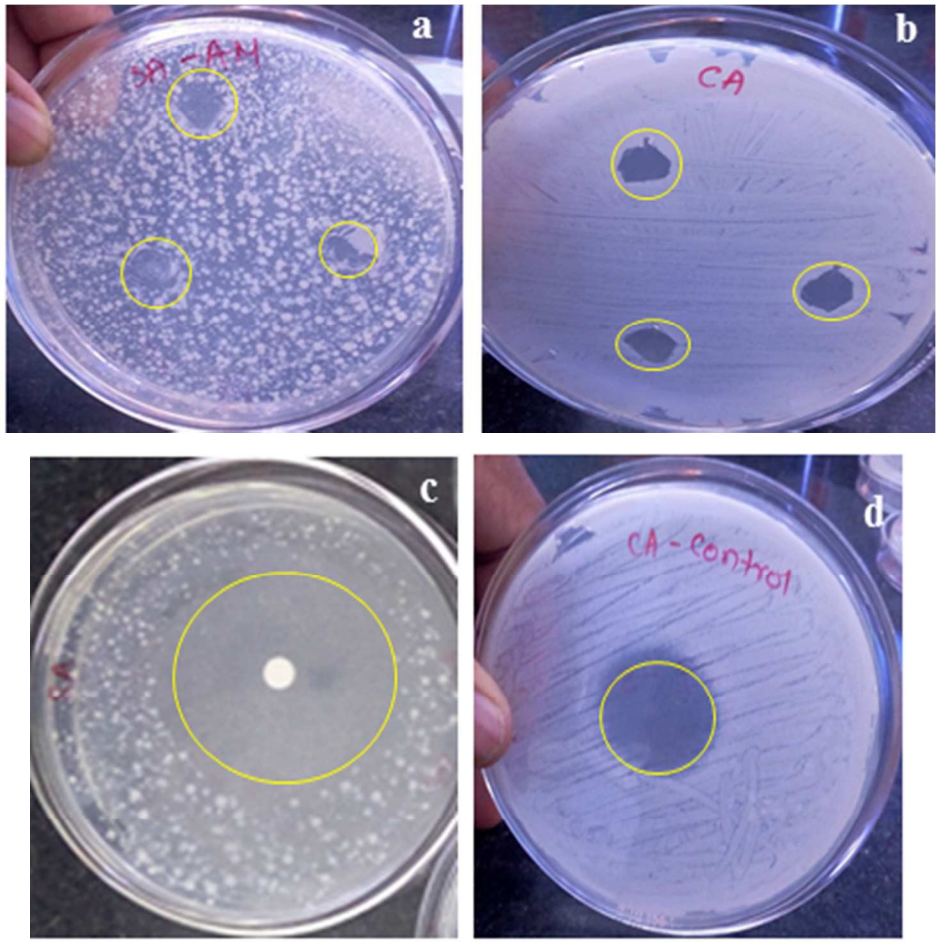

Fig.15 Representative agar plates showing a) few colonies of *Staphylococcus aureus*, b) complete inhibition of *Candida albicans*. The c) and d) are the standard Ciprofloxacin and Fluconazole inhibition of respective microbes.

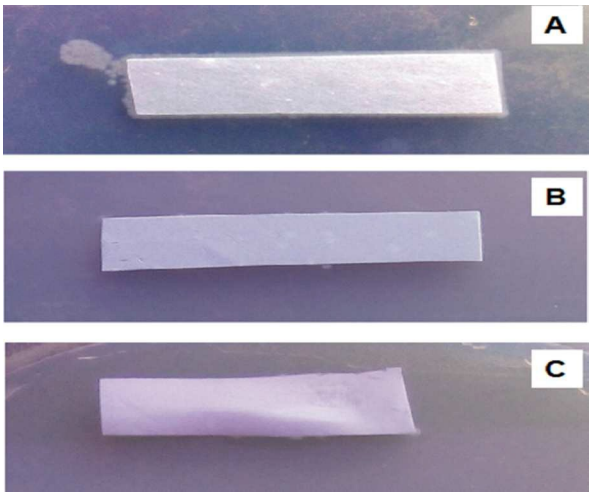

Fig.16 Membrane strips submerged in microbial culture was placed on the agar plates. A) colonies of *Candida albicans* around the control strip and no colonies on the HMM-1 (B) and HMM-2 (C) membrane strip respectively.

Table-1 - Composition of the casting solution

Membrane	PEI(g)	NMP(g)	MHNTs(g)	PVP	W_{MHNTs}*(wt%)
HMM-0	18	80	0	2	0
HMM-1	18	79.8	0.18	2	1
HMM-2	18	79.4	0.36	2	3
HMM-3	18	79.1	0.54	2	4

*W_{MHNTs} is the mass ratio of MHNTs to PEI.

Table-2 Properties of the prepared membranes

Membrane Code	Membrane Thickness(μm)	Porosity (%)	Hydraulic resistance (Kpa/Lm^{-2}h^{-1})
HMM-0	205	36.8	1.59
HMM-1	203	49.2	1.21
HMM-2	206	61.7	0.88
HMM-3	210	58.5	1.05

Table-3 : Filtration and antifouling performances of the membranes

Membrane code	Permeate Flux (L $m^{-2}h^{-1}$)			FRR and Fouling recovery (%)			
	J_{w1}	J_p	J_{w2}	FRR	R_t	R_r	R_{ir}
HMM-0	125.2	9.8	33.4	26.6	92.1	18.8	73.4
HMM-1	164.8	18.1	87.6	53.1	89.0	42.1	46.9
HMM-2	226.3	31.2	168.7	74.5	86.2	60.7	25.5
HMM-3	199.5	24.3	133.9	67.1	87.8	55.0	32.9

Table – 4

The reusability study for the heavy metal ion rejection

Cycles	Pb^{2+}		Cd^{2+}	
	PEUF	UF	PEUF	UF
1	79	34	73	27
2	76	31	71	25
3	74	32	69	26
4	75	33	70	25
5	76	31	68	27
6	75	32	69	25
7	76	33	68	26
8	75	33	68	25
9	74	34	67	26
10	75	35	69	27
11	75	34	66	26
12	76	33	67	26